Adika Maja Alif Utama^{1,2}, Ristiyanto Adiputra^{3*}, Aditya Rio Prabowo^{1,2**}, Jung Min Sohn⁴, Oleksiy Melnyk⁵, Svitlana Onyshchenko⁵, Nurul Muhayat¹, Wahyu Purwo Raharjo¹, Wibowo Wibowo¹, Yemi Kuswardi⁶

TOWARD ULTIMATE BENDING MOMENT OF MARINE-BASED STRUCTURES: MESH CONVERGENCE STUDY USING THE MST-3 BOX GIRDER

MAKSIMALNI MOMENT SAVIJANJA POMORSKIH KONSTRUKCIJA: STUDIJA KONVERGENCIJE MREŽE ELEMENATA NA PRIMERU MST-3 KUTIJASTOG PROFILA

Originalni naučni rad / Original scientific paper Rad primljen / Paper received: https://doi.org/10.69644/ivk-2025-02-0157

Adresa autora / Author's address:

¹⁾ Department of Mechanical Engineering, Universitas Sebelas Maret, Surakarta, Indonesia **email: aditya@ft.uns.ac.id

A.R. Prabowo https://orcid.org/0000-0001-5217-5943 N. Muhayat https://orcid.org/0000-0002-1086-7826

W.P. Raharjo https://orcid.org/0000-0001-7158-0004 W. Wibowo https://orcid.org/0000-0003-2849-7330

2) Laboratory of Design and Computational Mechanics, Faculty of Engineering, Universitas Sebelas Maret, Surakarta, Indonesia

3) Research Center for Hydrodynamics Technology, National

Research and Innovation Agency, Surabaya, Indonesia *email: ristiyanto.adiputra@brin.go.id,

R. Adiputra https://orcid.org/0000-0003-3630-9432

⁴⁾ Department of Naval Architecture and Marine Systems Engineering, Pukyong National University, Busan, Korea J.M. Sohn https://orcid.org/0000-0002-6495-479X

5) Department of Navigation and Maritime Safety, Odesa National Maritime University, Odesa, Ukraine

O. Melnyk https://orcid.org/0000-0001-9228-8459

S. Onyshchenko https://orcid.org/0000-0002-9660-1921

6) Department of Mathematics Education, Universitas Sebelas Maret, Surakarta, Indonesia Y. Kuswardi https://orcid.org/0009-0008-8101-9630

Keywords

- · box girder
- · bending moment
- · structural failure
- · finite element method

Abstract

In a nutshell, the box girder bending moment capacity is the sum of the bending moment capacity of each structural member. The main parameters affecting the box girder's longitudinal strength under pure bending moment and buckling are plate and column slenderness. Several methods have been proposed to assess the bending moment capacity of box girders. One method commonly known is the experiment method conducted by Nishihara using the 4-point bending method. The primary purpose of this study is to determine the effect of mesh convergence in Finite Element Analysis (FEA) on the experimental result. The finite element study has a principle similar to the experiment studies. The effect of the mesh convergence study is shown in the form of the error value towards the experimental result.

INTRODUCTION

Structural or hull failure in marine terms is defined as a condition when a structure cannot withstand the force acting on it. Many factors lead to accidents caused by hull failure on the marine base structure. Collision and contact are the commonly known reasons that lead to hull failure besides overload. According to the Marine Accidents Investigation Branch (MAIB), 1011 marine accidents occurred from 2012 until 2022, with two of the biggest reasons being collision and contact, which took about 42.4 %. Hull structures can be categorised as thin-walled structures. Previously, several assessments of thin-walled structures have been done to obtain the behaviour of structures under determined loading conditions /1-3/. Figure 1 shows collision and contact accidents, while Fig. 2 shows the number of accidents per year.

Ključne reči

- · kutijasti nosač
- moment savijanja
- lom konstrukcije
- · metoda konačnih elemenata

Izvod

Ukratko, kapacitet momenta savijanja kutijastog nosača je zbir kapaciteta momenata savijanja svakog elementa konstrukcije. Glavni parametri koji utiču na podužnu čvrstoću kutijastog nosača usled čistog momenta savijanja i izvijanja su vitkost ploče i vitkost stuba. Do sada je predloženo nekoliko metoda za procenu kapaciteta momenta savijanja kutijastog nosača. Jednu poznatu eksperimentalnu metodu je sproveo Nishihara koristeći metodu savijanja u 4 tačke. Glavni cilj ovog rada je određivanje uticaja konvergencije mreže elemenata u analizi konačnim elementima (FEA) na rezultat eksperimenta. Studija konačnim elementima ima sličan princip sa prethodnim eksperimentalnim studijama. Studija uticaja konvergencije mreže je predstavljena u obliku vrednosti greške u odnosu na rezultat eksperimenta.

Merchant Vessel(≥100Gt) Accidents between 2012-2022

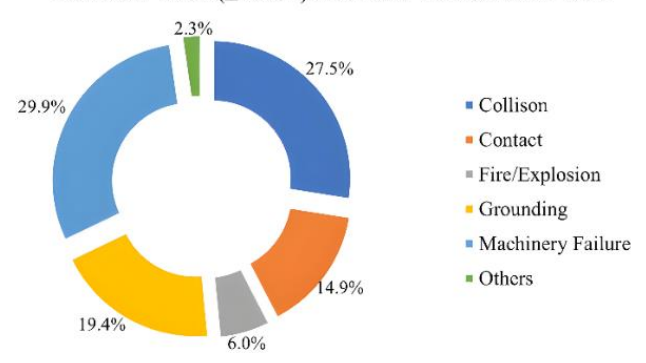


Figure 1. Percentage of collision and contact accidents.

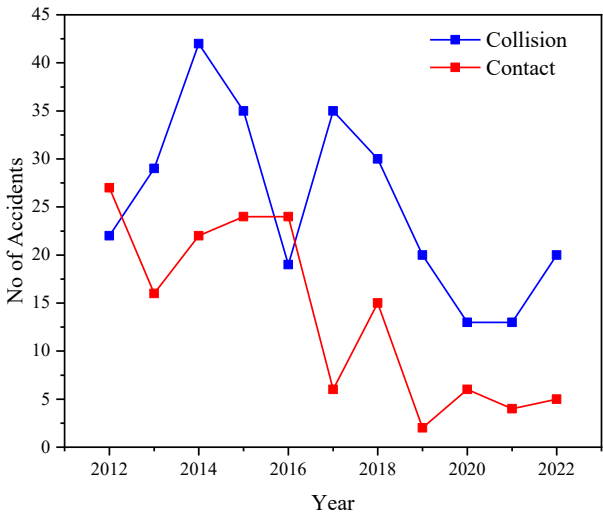


Figure 2. Comparison of the number of collisions and contacts.

The box girder is a key structural component of a vessel's hull. It is a vital structural element located longitudinally at the bottom of the ship; it enhances the hull's overall integrity, Fig. 3. It comprises several sub-components, including deck plating, side shell plating, bottom plating, and stiffen

ers, all of them meticulously arranged to form a closed loop that provides added rigidity and support.

The box girder plays an essential role in increasing the longitudinal strength of the vessel's hull which is crucial for maintaining structural stability under various loading conditions, whether in sagging or hogging scenarios. These conditions arise from the weight distribution and dynamic forces acting on the ship, such as waves and cargo loading which can compromise the vessel's structural integrity if not adequately addressed. In real-life applications, box girders are engineered to endure vertical bending moments which are further complicated by dynamic conditions such as slamming, /4/. Slamming creates localised stresses on the hull and introduces oscillatory motions that affect the overall distribution of forces, necessitating precise engineering to mitigate fatigue and fracture risks.

Besides that, a box girder can also be defined as a simplified representative of a vessel hull, Fig. 4. Box girders can be defined in that way because of the similarity of structure behaviour when subjected to a pure bending moment, /7/. Because of the simplicity of its geometry, the box girder is frequently used to test the longitudinal strength of the hull structure or to understand the failure mechanisms of the hull structure, /8/.

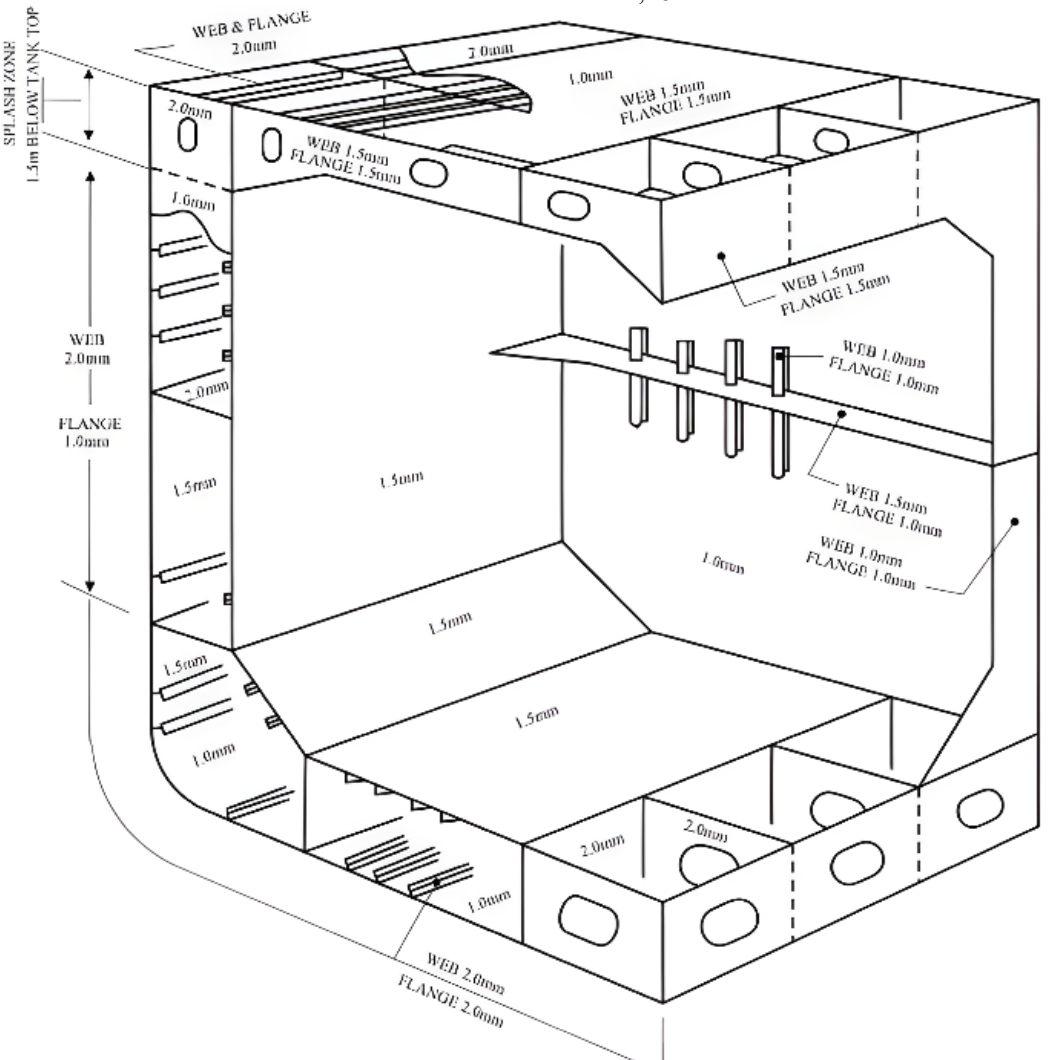


Figure 3. Position of the box girder within the hull structure, /5/.

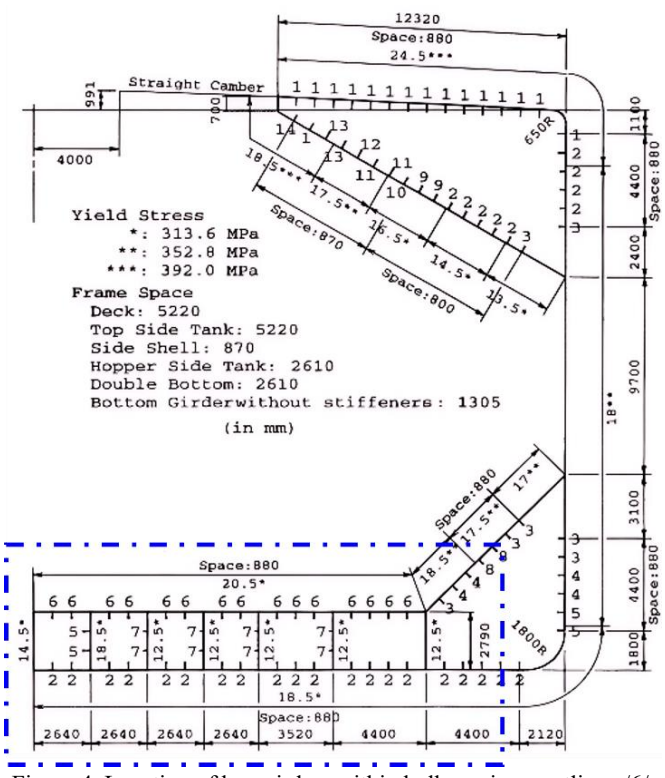


Figure 4. Location of box girders within bulk carrier scantlings /6/.

LITERATURE REVIEW

Previous research

Many studies have been conducted to analyse the ultimate bending strength of box girders, as presented in Table 1. Eldeen et al. /9/ conducted 4-point bending testing on the box girder to analyse the box girder characteristics, failure form, and maximum bending moment capacity of the box girder. Gordo and Soares, /10/ use HTS-690 material with 690 MPa of yield stress to achieve better efficiency in the structure. Gordo and Soares /11/ also assess the box girder by varying the distance between each transverse frame to

analyse the effect towards the ultimate bending moment capacity of the box girder. On the other hand, Park et al. /12/ experimented to analyse the ultimate bending moment capacity of a box girder that previously had severe fracture and denting. The fracture and denting in the box girder were generated using a drop hammer test with a knife edge and conical indenter. The location and the amount of indentation of the box girder have been varied; then, the result is compared with the base model (without fracture or indentation). The result of this experiment also varied with the Finite Element Method (FEM) which considers geometric imperfection of surface flatness deviation. Yamada and Takami /13/ also conducted an ultimate bending moment assessment of the box girder that sustains geometric imperfection; in this experiment, geometric imperfection is modelled with a hole on one side of the box girder. Eldeen et al. /14/ conducted an experiment to assess the ultimate bending moment of box girders that previously had corrosion. Three different levels of corrosion have been tested, including minor, moderate, and severe corrosion. The three levels are obtained through the application of different conditions before the examination of each model. The first model is submerged in high-temperature seawater without polarisation, the second in high-temperature seawater with polarisation, and the third in cold water with polarisation.

Calculation method

Generally, the calculation method of the ultimate bending moment on the box girder is divided into three primary methods: a direct method, progressive collapse analysis, and a numerical method. Caldwell first introduced the calculation method of the hull girder /15/. Caldwell first introduced the term 'plastic design,' and Strength Reduction Factor (SRF). Furthermore, this method has been improved by Paik /16/ using more reasonable assumptions about bending stress distribution on the cross-section area to calculate the ultimate strength of the hull girder.

Table 1. Research milestones towards the development of the box girder technology.

Authors	Year	Title	Method	Parameters
S. Nishihara	1983	Analysis of Ultimate Strength of Stiffened Rectangular Plate	Experimental method	Four different models of box girder Thickness variation
J. M. Gordo C. G. Soares	2009	Tests on ultimate strength of hull box girders made of high tensile steel	Experimental method	Plate and column slenderness Effectiveness of HTS 690
S. Saad-Eldeen Y. Garbatov C.G. Soares	2010	Experimental assessment of the ultimate strength of a box girder subjected to four-point bending moment	Experimental method	Comparison with empirical formula Plate and column slenderness Several loading cycles Release of residual stress
S. Saad-Eldeen Y. Garbatov C.G. Soares	2011	Experimental assessment of the ultimate strength of a box girder subjected to severe corrosion	Experimental method	Three levels of corrosion from different treatments Several loading cycles Release of residual stress
J.M. Gordo C.G. Soares	2014	Experimental analysis of the effect of frame spacing variation on the ultimate bending moment of box girders.	Experimental method	Effective structural modulus Analysis of elastic-plastic behaviour
Y. Yamada T. Takami	2015	Model test on the ultimate longitudinal strength of a damaged box girder		Hole on one side of the box girder Explicit non-linear finite element analysis
S.H. Park, S.H. Yoon T. Muttaqie, Q.T. Do S.R. Cho	2023	Effects of Local Denting and Fracture Damage on the Residual Longitudinal Strength of Box Girders		Denting and fracture by drop hammer test Residual longitudinal strength

Progressive collapse analysis was introduced as the 'incremental-iterative method,' commonly called Smith's method /17/. This method accounts for the load redistribution effects resulting from local failure of structural members. In this method, the complex cross-section of a hull girder is divided into three main components: plating, stiffeners, and hard corners. Each component's bending moment capacity is then calculated individually. Once the bending moment capacities of all structural elements are determined, these values must be integrated to obtain the entire structure's ultimate global bending moment capacity. The accuracy of PCM relies heavily on the load shortening and elongation (LSE) curve which can reliably simulate the progressive failure of ship structures. To enhance the accuracy in determining LSE data for box girders, Downes /18/ introduced a new approach using Finite Element Analysis (FEA).

Besides that, there is the Finite Element Method (FEM) introduced by Turner /19/ to evaluate the elasticity character of a complex shell structure. Structure stiffness is defined as the sum of stiffness from each structural member. In this method, a complex geometry is divided into more minor, interconnected elements; intersection vertices between each component are commonly known as nodes. In FEA terms, improving the number of nodes means decreasing the element size. In several simulations, this act usually improves accuracy or decreases the error value that may happen. Xu and Soares, /20/, conducted numerical analysis using FEA to simulate the effect of four kinds of stiffeners on stiffened panels under uniaxial compression.

The main parameters that affect the longitudinal structural strength of a box girder under pure bending moments, as well as its compression and buckling strength, are plate and column slenderness. These slenderness ratios are critical in predicting the girder's stability and strength and can be defined as presented in Eqs. (1) and (2).

$$\beta = \frac{b}{t} \sqrt{\frac{\sigma_0}{E}} , \qquad (1)$$

$$\lambda = \frac{a}{r} \sqrt{\frac{\sigma_0}{E}} , \qquad (2)$$

$$\lambda = \frac{a}{r} \sqrt{\frac{\sigma_0}{E}} \,, \tag{2}$$

where: b is defined as plate width between the stiffeners; t is plate thickness; a is the span between the transverse frame; and r is gyration radius of the cross-section that can be defined in Eq. (3),

$$r = \sqrt{\frac{I}{4}} \,, \tag{3}$$

where: I is defined as cross-section's inertia moment; and A is cross-sectional area. Zhang and Khan /21/ conducted an investigation about buckling and ultimate strength from 12 double hull oil tankers and ten bulk carriers, and found that the amount of plate slenderness β range about from 1.0 to 2.5, while the value of column slenderness λ ranged from about 0.25 to 0.95. Refer to Paik and Kim, /22/. There are seven modes of failure in stiffener plates. The most commonly encountered are flexural buckling and stiffener tripping. Equations (4) and (5) formulate the stiffener's strength

to withstand these conditions,

$$\Phi_b(\bar{\varepsilon}_i) = \Phi_{j0}(\bar{\varepsilon}_i) \frac{A_s + \Phi_w(\bar{\varepsilon}_i)bt}{A_s + bt},$$
(4)

$$\Phi_{t}(\bar{\varepsilon}_{i}) = \Phi_{t \min}(\bar{\varepsilon}_{i}) \frac{A_{s} + \Phi_{w}(\bar{\varepsilon}_{i})bt}{A_{s} + bt}.$$
 (5)

Besides that, the bending moment leads to compression on one side of the box girder, causing a loss of plate effectiveness. This reduction happens because compression can lead to local buckling which diminishes the plate's ability to carry loads effectively. To account for this, the remaining effective plate width under strain ε_i , can be calculated using Eq. (6),

$$\Phi_{w}(\overline{\varepsilon}_{i}) = \Phi_{e}(\overline{\varepsilon}_{i}) \left(\frac{2}{\beta} - \frac{1}{\beta^{2}}\right). \tag{6}$$

The effect of initial geometric imperfections has been considered as these influence the strength and stability of the beam, which in this study will be modelled as half waves due to weld distortion. As referenced by the International Ship and Offshore Structures Congress (ISSC), the expression value for these imperfections provides a standardised way to account for their effects in design calculations. It can be calculated sequentially using Eqs. (7), (8), and (9),

$$\omega_{opl} = A_0 \sin\left(\frac{m\pi x}{a}\right) \sin\left(\frac{\pi y}{b}\right), \tag{7}$$

$$\omega_{oc} = B_0 \sin\left(\frac{\pi x}{a}\right) \sin\left(\frac{\pi y}{b}\right), \tag{8}$$

$$\omega_{oc} = B_0 \sin\left(\frac{\pi x}{a}\right) \sin\left(\frac{\pi y}{b}\right),$$
 (8)

$$\omega_{os} = C_0 \left(\frac{z}{h_{\omega}}\right) \sin\left(\frac{\pi x}{a}\right),$$
 (9)

where: *m* as buckling periodic waves of a nominal value 3 (to fulfil the equation $a/b \le \sqrt{(m(m+1))}$; $B_0 = 0.0015a$; $C_0 =$ 0.0015a; and plate width between the longitudinal girder B = 3b. Smith suggested the A_0 value and divided it into three categories: slight, moderate, and severe, as seen in Eq.(10),

$$A_0 = \begin{cases} 0.025\beta^2 t & \text{for slight level} \\ 0.1\beta^2 t & \text{for average level} \end{cases}$$

$$0.3\beta^2 t & \text{for severe level}$$
(10)

According to the Japan Shipbuilding Quality Standard (JSQS), imperfection values are limited to 6 mm. Figure 5 illustrates the relationship between the square of plate slenderness multiplied by plate thickness.

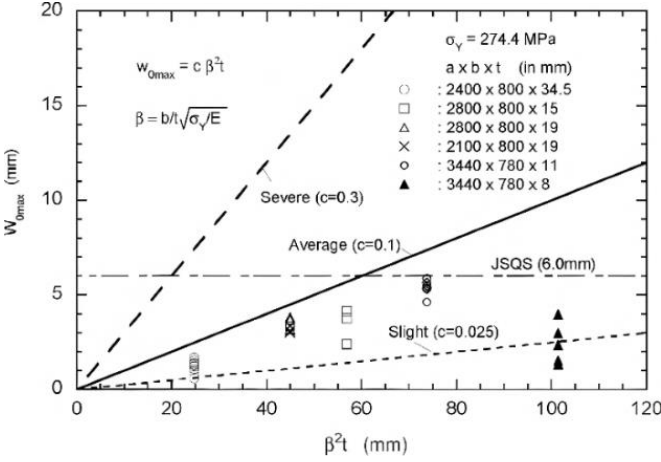


Figure 5. Relationship between the plate slenderness function toward the plate thickness /23/.

The ability of the box girder to withstand the bending moment acting on it can be defined as the sum of the abilities from each component of the box girder between two adjacent transverse frames, as presented by Eqs. (11)-(13),

$$M = \int_{A} (Z - Z_n) \sigma(z) dA = \sum_{i} (Z_i - Z_n) \sigma_i(Z_i) A_i, \quad (11)$$

$$\sigma(Z_i) = f(\varepsilon_i) \,, \tag{12}$$

$$\varepsilon_i = g(Z_i, Z_n) \,, \tag{13}$$

where: average stress σ on a stiffened panel can be defined as a function of average strain ε ; and depends on element location Z_i towards the neutral axis Z_n .

Model reference

The box girder model used is the MST-3 box girder. Nishihara first introduced this kind of box girder, /24/, as a representative of single-hull oil tankers (Fig. 6). In the conducted experiment, Nishihara has four kinds of different box girders. There are MST, MSD, MSB, and MSC, which in sequence represent the structures of single-hull oil tanker, double-hull oil tanker, bulk carrier, and container vessel. These four kinds of box girders will then be varied again in thickness into 3 mm and 4 mm, so there are eight models of the box girder in total. In this experiment, testing sections are connected to extended structures on both sides. An assembled model is then placed on top of a fixed roller, and an indenter roller that will move downward is placed a little

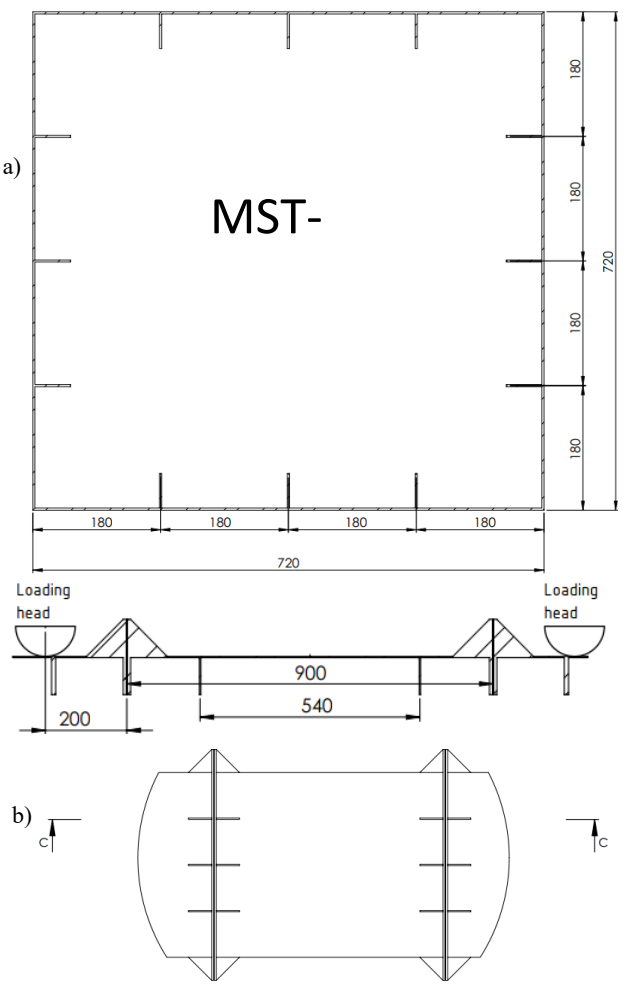


Figure 6. a) Cross section of box girder MST-3; and b) midspan testing section of Nishihara experiment.

further from the connection point; this testing method is commonly known as 4-point bend testing (Fig. 7). This method usually analyses the structure response under pure bending moment.

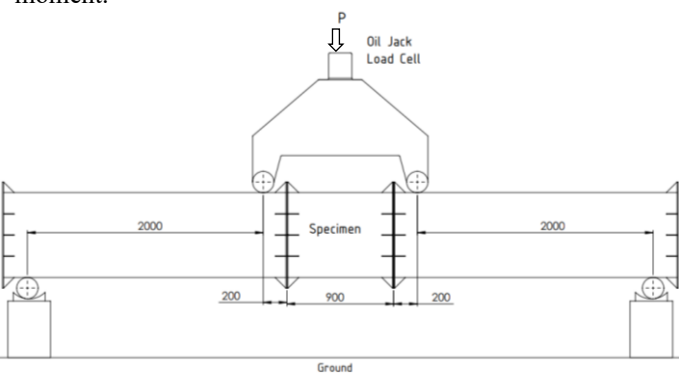


Figure 7. Nishihara 4-point bending test setup.

MST-3 consists of plates arranged to form a closed loop structure reinforced by a flat stiffener plate to enhance strength and stability. The plating and the stiffener share a similar thickness, ensuring uniformity in structural properties and load distribution. Mild steel is employed as the primary material for both components due to its favourable combination of strength, ductility, and cost-effectiveness. For the MST-3 model, the thickness of the steel used is 3 mm, balancing flexibility and durability for the intended application. In contrast, the MST-4 model utilises a slightly thicker steel plate, with a thickness of 4 mm.

METHODOLOGY

Table 2 outlines the specific material properties of the mild steel used in these models, including its yield strength, Poisson's ratio, and modulus of elasticity. It provides a comprehensive understanding of its mechanical behaviour under different loading conditions.

Table 2. Material properties of mild steel.

Parameter	Value
Density	7.8×10^{-6}
Young modulus	206920
Yield strength	287
Poisson ratio	0.277

The outcome of the assessment is the bending moment capacity of the MST-3 box girder, determined to be 5.88 × 10⁸ N/mm² as presented in Fig. 8. This value represents the maximal moment the structure can withstand before yielding or experiencing significant deformation. It is a critical parameter for evaluating the girder's structural integrity and performance under load. The calculated bending moment capacity provides insights into the box girder's ability to resist vertical forces. It is a benchmark for comparing alternative design approaches or material selections in future studies. By understanding the girder's bending capacity, engineers can ensure the safety and reliability of the structure in real-world maritime conditions, where dynamic forces such as slamming or wave impacts are constantly at play.

The present study employs FEA, utilising the Abaqus® Computer-aided Engineering (CAE) software to simulate the

structural behaviour under pure bending moments. The FEA methodology replicates the geometry of the physical testing setup, incorporating key components such as the fix roller, the indenter roller, and the main structure. The main structure consists of a midspan testing section representing the critical region of interest and two extended structures on either side, connected by bolts to ensure proper load transfer during testing, Fig. 9. These extended sections help simulate realistic boundary conditions and prevent premature failure at the test section ends, Fig. 10.

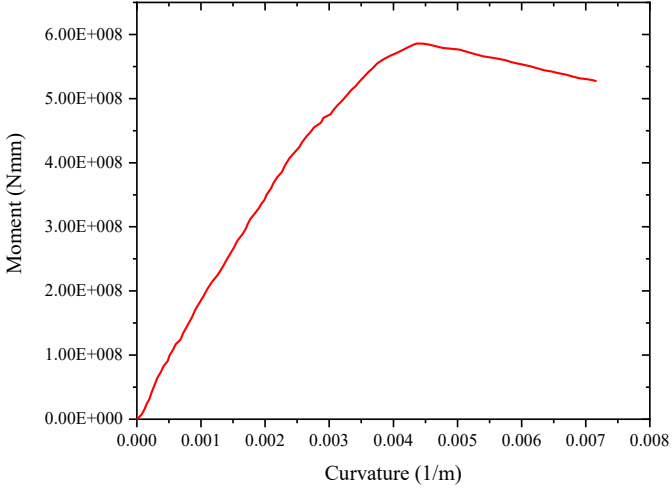


Figure 8. Load-curvature curve of MST-3 box girder conducted by Nishihara /24/.

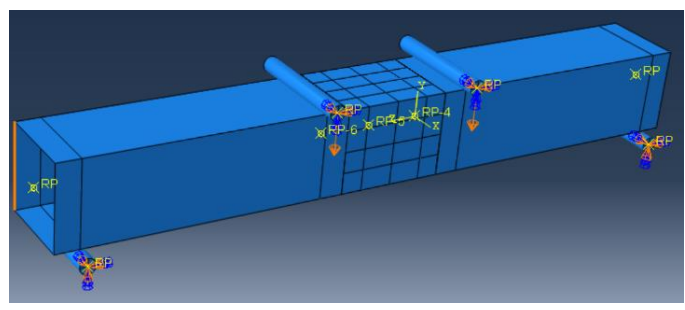


Figure 9. FEA model of 4-point bending test.

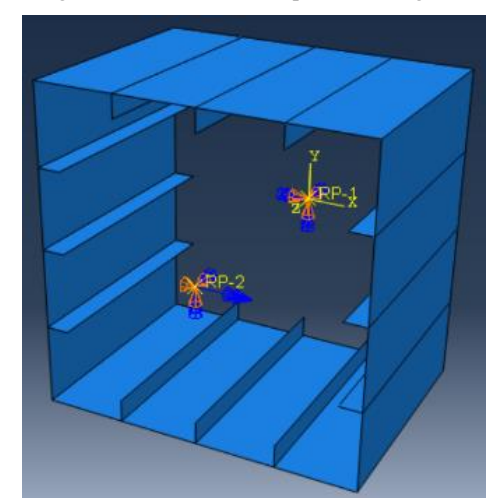


Figure 10. Boundary conditions of simplified approach.

The fixed rollers are constrained during the simulation to prevent translation or rotation. The main structure is carefully positioned between the fix and indenter rollers to mimic the test conditions. The loading mechanism is applied through a controlled downward movement of the indenter roller until a predetermined displacement is reached. This allows the structural response under pure bending moments to be closely monitored, capturing critical behaviours.

This study presents a simplified approach. The proposed method is expected to offer improved efficiency, reducing computational time and resource utilisation. The method involves modelling a single component, namely the midspan testing section. The loading is not defined as indenter displacement but rather as a moment load at a reference point previously anchored to the midspan edges on one side. A similar connection is applied on the other side to create a fixed constraint. The obtained variables are extracted from both reference points, Fig. 11.

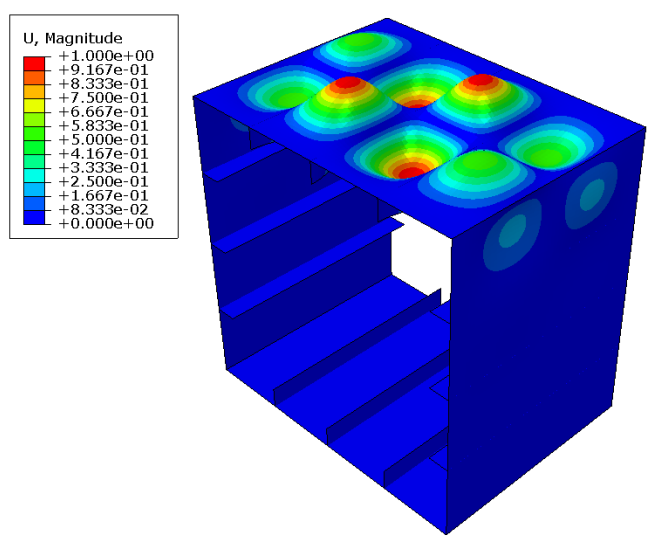


Figure 11. Stiffeners tripping as the initial geometric imperfection of the midspan (deformation scale = 72).

Before assessing the bending moment, initiating the initial geometric imperfection of the midspan section is crucial. This step is essential for ensuring that the model accurately reflects real-world conditions, where various factors such as material inconsistencies, manufacturing defects, or residual stresses can influence the structural behaviour and experimental outcomes. In this study, the initial geometric imperfection is modelled as several halfwaves representing geometry distortion due to the fabrication process using Abaqus® CAE software, where a linear perturbation buckle procedure is employed to introduce a predefined buckle pattern. This method allows for a realistic simulation of imperfections in structural elements. After the initiation of this imperfection, the resulting deformed shape can be visualised as several half-waves that appear along the plating and stiffeners which are the characteristic of stiffener tripping or stiffener web buckling, /25-32/. Then, this imperfection will vary the magnitude which we can call the Degree of Imperfection (DOI), into several values, including 0.1 %, 0.5 %, 5 %, and 10 % which satisfy the predefined categories suggested by Smith in Eq. (10). These buckling modes are commonly observed in practice, especially in thin-walled structures subjected to compressive forces. The initiation of these geometric imperfections provides a critical foundation for accurate bending moment assessment, as it allows the model to account for imperfections that may trigger early failure or instability.

RESULTS AND DISCUSSION

Once the setup is finalised, each method's results are systematically compared against the Nishihara curve which is used as a reference benchmark to evaluate the effectiveness of the various approaches. The resulting comparison graphs (Fig. 12) clearly illustrate that the simplified approach consistently outperforms the entire model in terms of accuracy, yielding a significantly smaller error value of 7.91 %. In contrast, the model displays a noticeably higher error value of 21.94 %. This stark contrast indicates that the simplified model captures the system's essential features with greater precision and is a more efficient approach to minimising computational discrepancies.

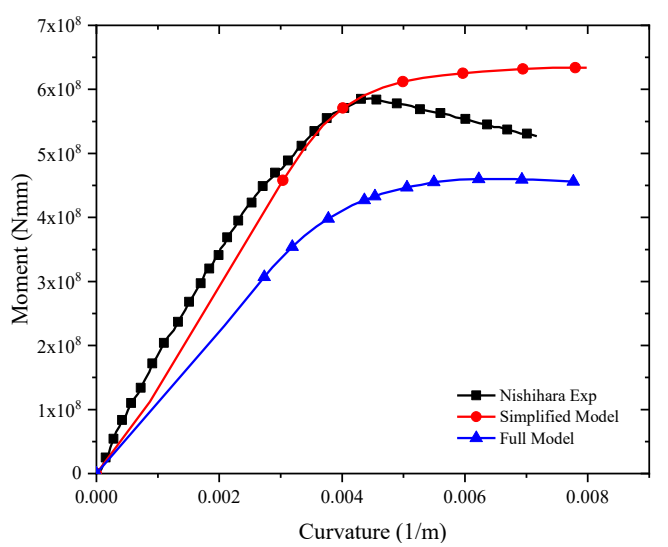


Figure 12. Comparison curve of proposed methods.

As a result, the simplified model will be adopted as the foundational framework for all subsequent convergence studies, ensuring that future analyses are both accurate and computationally efficient. Relying on this model will streamline further investigations, enabling a more precise evaluation of model behaviour across various mesh sizes and other parameters.

After the necessary parameters are defined, a mesh convergence study is conducted to evaluate the maximal bending moment capacity of the MST-3 box girder. This convergence study is critical in ensuring that the chosen mesh size provides accurate results while maintaining computational efficiency. It involves testing a range of mesh sizes to determine the optimal balance between accuracy and performance. The study begins with mesh sizes varying from 9 to 54 mm, incremented at 5 mm intervals, followed by a more refined range from 9 to 5 mm, incremented at 1 mm intervals to capture finer details in the model. This approach allows for a comprehensive evaluation of how different mesh densities influence the calculated bending moment and the overall accuracy of the simulation. As the mesh size decreases, the solution is expected to become more precise, but at the cost of increased computational resources and time.

The curves in Figs. 13 and 14 show the result from the simulation conducted in several mesh sizes and are compared to the result from the Nishihara experiment. Figure 15 shows mesh size vs. error.

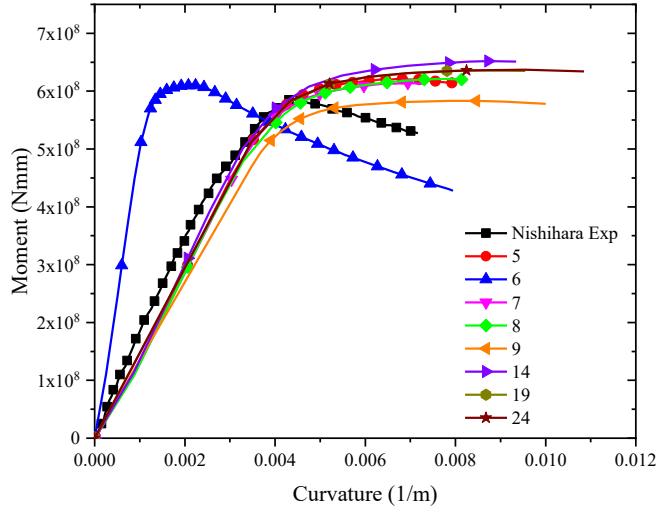


Figure 13. Mesh convergence result, mesh size 5-24.

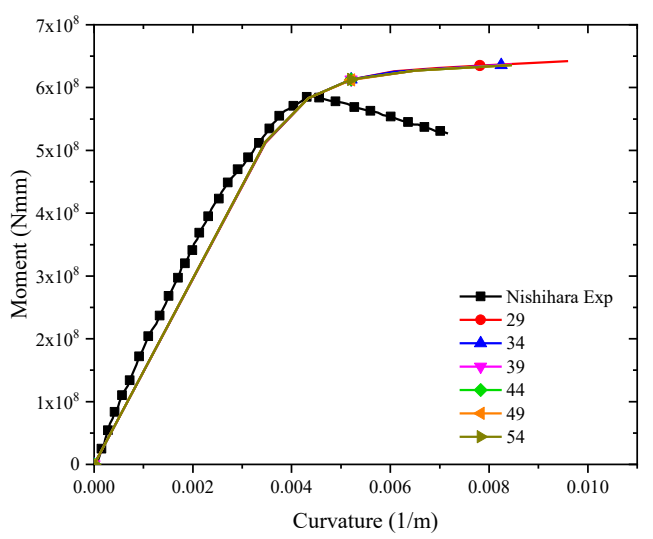


Figure 14. Mesh convergence result, mesh size 29-54.

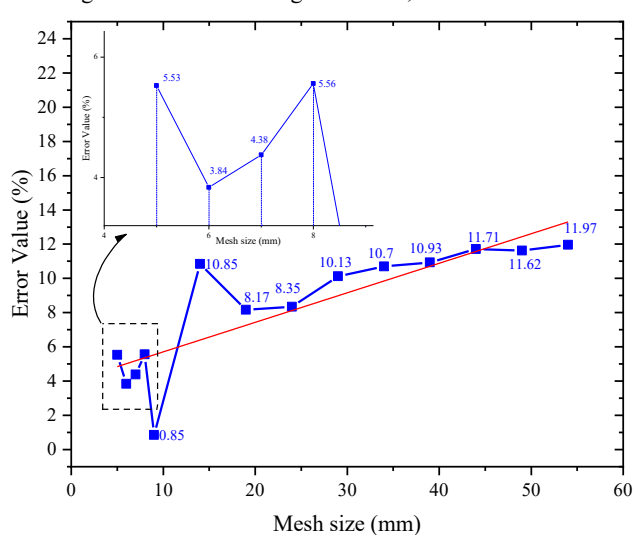


Figure 15. Relationship between mesh size and error value.

The graph in Fig. 16 illustrates mesh size and error value relations, visually representing the deviation of each mesh size towards the experimental value, seen as a dimensionless value. Generally, it can be observed that a finer mesh size tends to result in a smaller error value that indicates improved accuracy in computational results. This occurs because a finer mesh allows for a more detailed representation of the geometry and stress distribution, capturing subtle structural behaviours that might be missed with coarser meshes. However, achieving this increased precision comes at the cost of significantly higher computational resources which can become prohibitive in large-scale or real-time applications. This trade-off between accuracy and computational efficiency is a key consideration when determining the appropriate mesh size for a given analysis.

The study reveals that the optimal mesh size for minimising error is 9 mm. The error value is sufficiently low, at 0.85 %, ensuring reliable results between the experimental and numerical studies. Although higher mesh size, starting from 29 mm has reached the convergence phase, it will not be selected because the error remains stable at more than 10 %, leading to overestimation.

Once all the necessary setup procedures are completed, initial geometric imperfections can be generated to observe the effect of initial geometric imperfection toward the experimental value. This step systematically compares several degrees of imperfection (DOI), beginning with a small value of 0.1 and progressively increasing to 0.5, 5, and ultimately, 10. The present stage of the experiment is essential in predicting the imperfection of MST3 during experimental testing. After simulating the model for each DOI value, the outcomes are meticulously compared with the experimental results from the Nishihara experiment. This comparison is crucial for determining which degree of imperfection most closely aligns with experimental data, thereby validating the accuracy of the FEA model. From the comparison curve shown in Fig. 16, it becomes clear that a DOI value of 10 yields the most precise results, exhibiting only a minimal difference of 0.83 % from experimental findings. This starkly contrasts the other DOI values which show more significant deviations, highlighting the importance of choosing an appropriate DOI for accurate modelling.

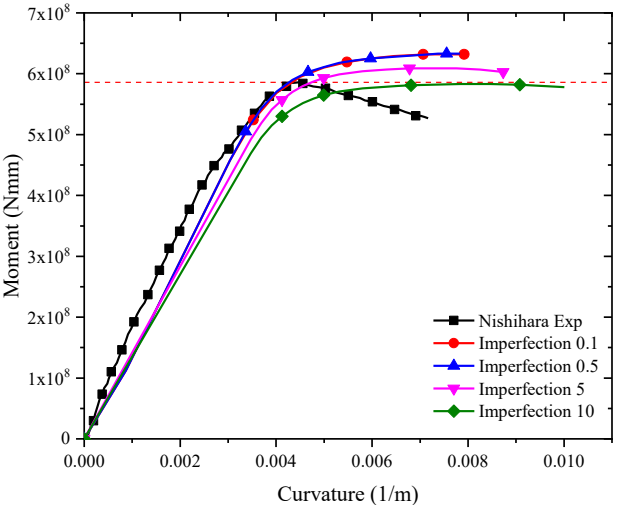


Figure 16. Comparison curves from several values of DOI.

In general, the stress and displacement contours of the structure when utilising a 9 mm mesh size can be seen sequentially in Figs. 17 and 18, providing a comprehensive visualisation of how the applied loads affect the material.

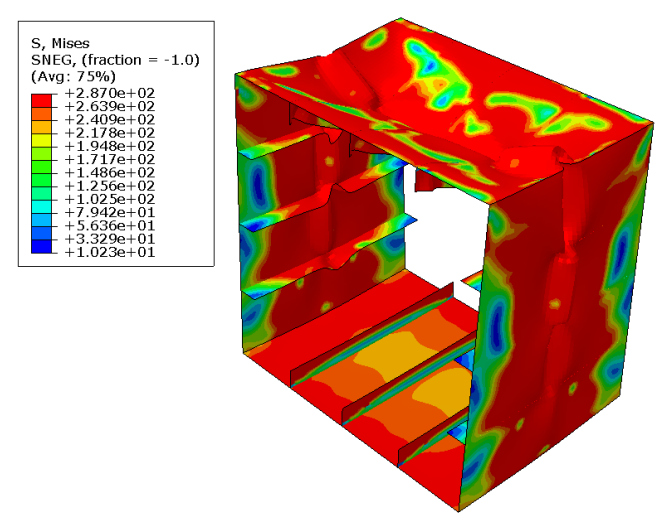


Figure 17. Stress contour of the midspan structure.

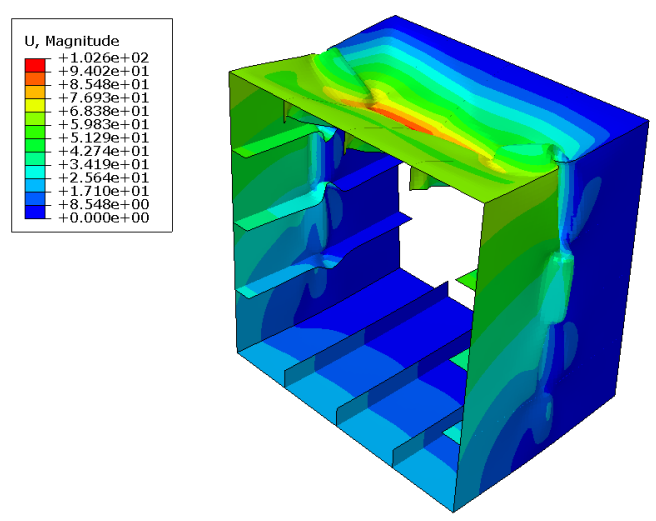


Figure 18. Displacement contour of the midspan structure.

These contours illustrate stress distribution across different regions of the structure, highlighting areas of potential weakness or failure and depicting how much the structure deforms under load. By analysing these contours, we can gain valuable insights into structural performance, enabling us to make informed decisions regarding design optimisation and safety assessments.

CONCLUSIONS

The simulation conducted aims to propose a compatible Finite Element Method (FEM) through a mesh convergence study with geometric imperfection initiation that has been validated using experimental results. From the results of the simulation model described in this article, some conclusions can be drawn as follows.

Generally, a finer mesh size tends to result in smaller error values, aligning with traditional expectations in computational modelling. However, this experiment reveals a significant deviation from this trend, mainly when the mesh size is less than 9 mm. The error values increase in such cases, indicating nonlinearities contradicting the established theory. This unexpected behaviour suggests that further investigation is needed to understand the underlying causes of this phenomenon.

The study emphasizes that several preprocessing steps, particularly initiating geometric imperfections, must be undertaken to ensure that the finite element analysis (FEA) setup aligns closely with experimental conditions. This step is crucial, as it allows for more accurate comparisons between FEA results and experimental findings, ultimately leading to more reliable and meaningful conclusions.

The proposed simplified method demonstrates a smaller error value and improves resource efficiency compared to the full-size method. This finding highlights the potential for streamlined approaches in structural analysis without sacrificing accuracy, making it a valuable contribution to the field.

Further studies are necessary to understand the factors influencing the observed nonlinear responses fully. These investigations will help identify the specific parameters that contribute to the nonlinearity and guide the refinement of the FEM approach. By exploring these complexities, future research can enhance the accuracy and reliability of simulations in structural engineering, ensuring that they effectively mirror real-world behaviours and responses.

ACKNOWLEDGEMENTS

This work is supported by the RKAT PTNBH Universitas Sebelas Maret, year 2025, under the research scheme of 'Penelitian Fundamental B' (PFB-UNS) with research grant/contract no. 369/UN27.22/PT.01.03/2025. The authors highly acknowledge this support.

REFERENCES

- 1. Đurđević, Đ., Đurđević, A., Andelić, N., et al. (2022), Strength and reliability of open cross-sections thin wall beams in a raft load-bearing structure, Struct. Integr. Life, 22(3): 335-338.
- Đurđević, Đ., Anđelić, N., Đurđević, A., et al. (2023), Thinwalled omega profile exposed to constrained torsion-analytical and numerical stress and strain calculation, Struct. Integr. Life, 23(2): 225-229.
- 3. Đurđević, Đ., Anđelić, N., Milošević-Mitić, V., et al. (2019), Influence of encastering on thin-walled cantilever beams with U and Z profiles on the magnitude of equivalent stress and deformation, Struct. Integr. Life, 19(3): 251-254.
- Shi, G.-J., Wang, D.-Y., Wang, F.-H., Cai, S.-J. (2023), Analysis of dynamic response and ultimate strength for box girder under bending moment. J Mar. Sci. Eng. 11(2): 373. doi: 10.3390/jms e11020373
- Zareei, M.R., Iranmanesh, M. (2018), Optimal risk-based maintenance planning of ship hull structure, J Mar. Sci. Appl. 17(4): 603-624. doi: 10.1007/s11804-018-00058-2
- Ohtsubo, H., Sumi, Y. (Eds.), Proceedings of the 14th Internaional Ship and Offshore Structures Congress, Vol. 1-3, Elsevier Science, 2000.
- Guedes Soares, C., Chen, N.Z., Santos, F.M., Santos, C. (2007), *An experimental and numerical study on GFRP box girder under pure bending*, In: C. Guedes Soares, P.K. Das (Eds.), Advance- ments in Marine Structures, Taylor & Francis Group, London, 2007, pp.385-389. ISBN 978-0-415-43725-7

- 8. Akhras, G., Gibson, S., Yang, S., Morchat, R. (1998), *Ultimate strength of a box girder simulating the hull of a ship*, Can. J Civ. Eng. 25(5): 829-843. doi: 10.1139/198-017
- Eldeen, S., Garbatov, Y., Guedes Soares, C. (2010), Experimental assessment of the ultimate strength of a box girder subjected to four-point bending moment, In: S.F. Estefen, I.P. Pasqualino, and S.H. Sphaler (Eds.), Proc. 11th Int. Symp. on Practical Design of Ships and Other Floating Struct. (PRADS 2010), Rio de Janeiro, Brazil, 2010, COPPE-URRJ, 2010, pp.1134-1143.
- 10. Gordo, J.M., Guedes Soares, C. (2009), Tests on ultimate strength of hull box girders made of high tensile steel, Mar. Struct. 22 (4): 770-790. doi: 10.1016/j.marstruc.2009.07.002
- Gordo, J.M., Guedes Soares, C. (2014), Experimental analysis of the effect of frame spacing variation on the ultimate bending moment of box girders, Mar. Struct. 37: 111-134. doi: 10.1016/ j.marstruc.2014.03.003
- 12. Park, S.-H., Yoon, S.-H., Muttaqie, T., et al. (2023), Effects of local denting and fracture damage on the residual longitudinal strength of box girders, J Mar. Sci. Eng. 11(1): 76. doi: 10.339 0/jmse11010076
- Yamada, Y., Takami, T. (2015), Model test on the ultimate longitudinal strength of a damaged box girder, In: C. Guedes Soares and R.A. Shenoi (Eds.), Analysis and Design of Marine Structures V, CRC Press, London, 2015, pp. 435-444.
- Saad-Eldeen, S., Garbatov, Y., Guedes Soares, C. (2011), Experimental assessment of the ultimate strength of a box girder subjected to severe corrosion, Mar. Struct. 24(4): 338-357. doi: 10.1016/j.marstruc.2011.05.002
- 15. Caldwell, J.B. (1965), *Ultimate longitudinal strength*, Trans. Roy. Inst. Naval Arch. Quart. Trans. 107(3): 411-430.
- Paik, J.K., Kim, D.K., Park, D.H., et al. (2013), Modified Paik-Mansour formula for ultimate strength calculations of ship hulls, Ships Offshore Struct. 8(3-4): 245-260. doi: 10.1080/17445302 .2012.676247
- Smith, C.S. (1977), Influence of local compressive failure on ultimate longitudinal strength of a ship's hull, In: N.Z. Gakkai (Ed.), Proc. Int. Symp. on Practical Design in Shipbuilding (PRADS 1977), Tokio, Japan, 1977, Society of Naval Architects of Japan, 1977.
- 18. Downes, J., Tayyar, G.T., Kvan, I., Choung, J. (2017), *A new procedure for load-shortening and -elongation data for progressive collapse method*, Int. J Nav. Arch. Ocean Eng. 9(6): 705-719. doi: 10.1016/j.ijnaoe.2016.10.005
- Turner, M.J., Clough, R.W., Martin, H.C., Topp, L.J. (1956), Stiffness and deflection analysis of complex structures, J Aeronaut. Sci. 23(9): 805-823.
- Xu, M.C., Guedes Soares, C. (2012), Numerical assessment of experiments on the ultimate strength of stiffened panels, Eng. Struct. 45: 460-471. doi: 10.1016/j.engstruct.2012.06.045
- 21. Zhang, S., Khan, I. (2009), Buckling and ultimate capability of plates and stiffened panels in axial compression, Mar. Struct. 22(4): 791-808. doi: 10.1016/j.marstruc.2009.09.001
- 22. Paik, J.K., Kim, B.J. (2002), Ultimate strength formulations for stiffened panels under combined axial load, in-plane bending and lateral pressure: a benchmark study, Thin-Walled Struct. 40(1): 45-83. doi: 10.1016/S0263-8231(01)00043-X
- Fujikubo, M., Yao, T., Khedmati, M.R., et al. (2005), Estimation of ultimate strength of continuous stiffened panel under combined transverse thrust and lateral pressure Part 1: Continuous plate, Mar. Struct. 18(5-6): 383-410. doi: 10.1016/j.marstruc.2005.08.004
- 24. Nishihara, S. (1983), Analysis of ultimate strength of stiffened rectangular plate (4th report) on the ultimate bending moment of ship hull girder, J Soc. Nav. Arch. Jpn. 154: 367.

- 25. Zhang, Q., Yang, H., Wu, S., et al. (2023), A study on the ultimate strength and failure mode of stiffened panels, J Mar. Sci. Eng. 11(6): 1214. doi: 10.3390/jmse11061214
- 26. Song, S., Ehlers, S., Braun, M., et al. (2025), '3Co principle' for fidelity assessment for bulb flat models in ship structural analysis, Res. Eng. 25: 103779. doi: 10.1016/j.rineng.2024.103779
- 27. Hanif, M.I., Adiputra, R., Prabowo, A.R., et al. (2023), Assessment of the ultimate strength of stiffened panels of ships considering uncertainties in geometrical aspects: Finite element approach and simplified formula, Ocean Eng. 286(Part 1): 115 522. doi: 10.1016/j.oceaneng.2023.115522
- 28. Sarwoko, A.R.K., Prabowo, A.R., Ghanbari-Ghazijahani, T., et al. (2024), *Buckling of thin-walled stiffened panels in transportation structures: Benchmarking and parametric study*, Eng. Sci. 30: 1137. doi: 10.30919/es1137
- 29. Prabowo, A.R., Ridwan, R., Tuswan, T., et al. (2024), Crushing resistance on the metal-based plate under impact loading: A systematic study on the indenter radius influence in grounding accident, Appl. Eng. Sci. 18: 100177. doi: 10.1016/j.apples.202 4.100177
- 30. Prabowo, A.R., Ridwan, R., Muttaqie, T. (2022), On the resistance to buckling loads of idealized hull structures: FE analysis on designed-stiffened plates, Designs, 6(3): 46. doi: 10.339 0/designs6030046
- Li, D., Chen, Z. (2025), Generalized closed-form formulae for characterizing the ultimate strength envelope of ship stiffened panels subjected to combined biaxial compression and lateral pressure, Mar. Struct. 102: 103789. doi: 10.1016/j.marstruc.20 25.103789
- 32. Han, J., Li, S., Zhang, A.-M. (2023), Applications of bond-based cohesive peridynamics method (CPDM) to simulate inelastic fracture of stiffened plates in ship hull structures, Comp. Struct. 286: 107108. doi: 10.1016/j.compstruc.2023.107108
- © 2025 The Author. Structural Integrity and Life, Published by DIVK (The Society for Structural Integrity and Life 'Prof. Dr Stojan Sedmak') (http://divk.inovacionicentar.rs/ivk/home.html). This is an open access article distributed under the terms and conditions of the Creative.commons Attribution-NonCommercial-NoDerivatives 4.0 International License